

RSC Advances



This is an *Accepted Manuscript*, which has been through the Royal Society of Chemistry peer review process and has been accepted for publication.

Accepted Manuscripts are published online shortly after acceptance, before technical editing, formatting and proof reading. Using this free service, authors can make their results available to the community, in citable form, before we publish the edited article. This *Accepted Manuscript* will be replaced by the edited, formatted and paginated article as soon as this is available.

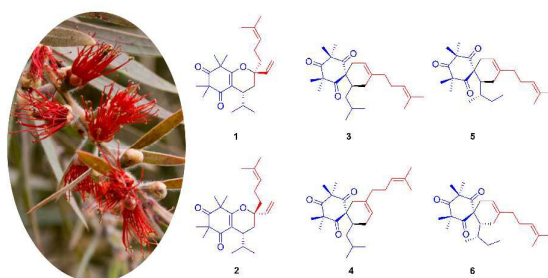
You can find more information about *Accepted Manuscripts* in the [Information for Authors](#).

Please note that technical editing may introduce minor changes to the text and/or graphics, which may alter content. The journal's standard [Terms & Conditions](#) and the [Ethical guidelines](#) still apply. In no event shall the Royal Society of Chemistry be held responsible for any errors or omissions in this *Accepted Manuscript* or any consequences arising from the use of any information it contains.

Graphical Abstract

Calliviminones C-H: Six New Hetero- and Carbon-Diels-Alder Adducts with Unusual Skeletons from the Fruits of *Callistemon viminalis*

Lin Wu, Jun Luo, Xiao-bing Wang, Rui-jun Li, Ya-long Zhang and Ling-Yi Kong*



Calliviminones C-H: Six New Hetero- and Carbon-Diels-Alder Adducts with Unusual Skeletons from the Fruits of *Callistemon viminalis*

Lin Wu, Jun Luo, Xiao-bing Wang, Rui-jun Li, Ya-long Zhang and Ling-Yi Kong^{*}

State Key Laboratory of Natural Medicines, Department of Natural Medicinal Chemistry, China Pharmaceutical University, 24 Tong Jia Xiang, Nanjing 210009, People's Republic of China

ABSTRACT

Calliviminones C-H (**1-6**), six novel Diels-Alder adducts of polymethylated phloroglucinol derivative and acyclic monoterpene (myrcene), were isolated from the fruits of *Callistemon viminalis*. Their structures were elucidated on the basis of extensive analysis of NMR spectroscopic data and calculated electronic circular dichroism spectra. Compounds **1** and **2** were the first examples of polymethylated phloroglucinol derivative connected with myrcene in hetero-Diels-Alder manner and **3-6** were carbon-Diels-Alder adducts featuring an unusual core of spiro-[5.5]undecene. Bioactivity scan indicated that **2-6** showed moderate inhibition on nitric oxide production in lipopolysaccharide-induced RAW264.7 macrophages.

Keywords: *Callistemon viminalis*; Diels-Alder adducts; Phloroglucinol; Nitric oxide

INTRODUCTION

Acylphloroglucinols are prominent secondary metabolites of the family Myrtaceae, and the shared phloroglucinol core of these derivatives is usually substituted by mono- or sesquiterpenoid moieties.¹ *Callistemon viminalis* (Myrtaceae), a native of Australia, has also been cultivated in the south of China, and whose leaves are commonly used as a traditional Chinese medicine (TCM) to treat cold and arthralgia.² Several biological activities have been reported for extracts of this genus plant, and some have exhibited insecticidal and antibacterial properties.³⁻⁵

In our previous studies, two novel monoterpene-based adducts were isolated from the title plant, which were also synthesized successfully based on the hypothesis of biosynthetic pathway in Diels-Alder manner.⁶ The unique and abundant structural features of Diels-Alder adducts prompted us to do a further investigation on this plant. As a result, six novel adducts of polymethylated phloroglucinol (β -triketone) derivative with monoterpene (myrcene) unit linked in two different manner were isolated from the fruits of *C. viminalis* collected in Guangzhou of China. The structures of these new compounds were established by analysis of their NMR spectroscopic data and experimental and calculated electronic circular dichroism (ECD) spectra. Compounds **1** and **2** are novel hetero-Diels-Alder adducts of β -triketone and acyclic monoterpene (myrcene) units, while **3-6** are carbon-Diels-Alder adducts of these two units possessing an unusual spiro-[5.5] undecene skeleton. Furthermore, Compounds **5** and **6** were the first examples of such Diels-Alder type adduct to be obtained as a single diastereomer, respectively, and their absolute configurations were determined by calculated ECD spectra. Bioactivity scan indicated that **2-6** showed inhibitory activities on nitric oxide production in LPS-induced RAW264.7 macrophages with IC₅₀ values ranging from 19.9 to 48.6 μ M. Herein, we report the isolation, structural elucidation, the plausible biosynthetic pathway and biological activities of these novel compounds.

RESULTS AND DISCUSSION

Calliviminone C (**1**) was obtained as colorless gum and designated with an elemental formula of $C_{24}H_{36}O_3$ by HRESIMS at m/z 373.2738 from the $[M+H]^+$ ion. From an inspection of its 1H and ^{13}C NMR spectra, **1** was found to possess a disubstituted isobutyl side chain [δ_H 2.62 (1H, m), 2.71 (2H, m) and two doublet methyls at 0.95 (3H, d, $J=7.0$) and 0.60 (3H, d, $J=7.0$)] and a tetramethylcyclohexenedione unit^{7, 8} [δ_H 1.44, 1.40, 1.31, 1.30 (each 3H, s) and δ_C 213.6, 197.7, 170.7, 112.5, 55.6, 48.3, 25.8, 25.3, 25.2, 24.0]. Consideration of the 1D NMR spectra and the HSQC spectrum of **1**, besides the signals arising from tetramethylcyclohexenedione unit and the disubstituted isobutyl group, 10 carbon signals including two quaternary carbons (one olefinic carbon at δ_C 132.1), two olefinic carbons (δ_C 123.9, 139.1), four methylenes (one olefinic carbon at 115.4) and two methyls were observed. The aforementioned data implied that compound **1** was an adduct of tetramethylcyclohexenedione and monoterpene.^{1, 8} The HMBC correlations (Fig. 2) of Me-10'/C-7', H-6'/C-7', C-3', H-5'/C-6', C-4' and H-1'/C-3' suggested the presence of an acyclic monoterpene of the myrcene type.⁶ The disubstituted isobutyl group was linked to C-6 of tetramethylcyclohexenedione nucleus, as judged from the correlations between H-7 and C-6, C-1 in the HMBC spectrum. The linkage of myrcene and isobutyl tetramethylcyclohexenedione moieties was determined to be a C–C bond between C-4' and C-7 and an oxygen atom between C-1 and C-3', according to the HMBC correlation of H-7/C-4' and the obvious downfield shift of C-3'. The above deductions established the planar structure of **1**. From a biosynthetic point of view, compound **1** could be derived from isobutyldiene syncarpic acid (β -triketone) and myrcene via hetero-Diels–Alder reaction, which is first example in natural products.

The relative configuration of compound **1** was established by NOE experiments. Significant NOE enhancements (Fig. 2) of H-4' (δ_H 1.89) with H-7 and H-2' indicated that H-7 and the fragments of C-1' to C-2' were oriented on the same side of the

dihydropyran ring and were arbitrarily designated as the β -orientation. Compound **1** was isolated as a racemic mixture, which was evident by the lack of optical rotation and electronic circular dichroic (ECD) Cotton effects. Therefore, the structure of **1** was depicted as shown.

Calliviminone D (**2**) was purified as a colorless gum, and gave $[M+H]^+$ peak at m/z 373.2735 (HRESIMS) for the molecular formula $C_{24}H_{36}O_3$. The close similarity of the UV, IR, and NMR spectroscopic data of **2** and **1** suggested these compounds to be close analogues. Its NMR data were similar to those of **1** except for the obviously chemical shifts of H-2' ($\Delta\delta$ 0.3), C-1' ($\Delta\delta$ -1.7) and C-5' ($\Delta\delta$ -5.7). The HMBC correlations of H-7 with C-4' and C-6, H-4' with C-5', H-1' with C-3', and H-5' with C-6' suggested that **2** had the same planar structure as **1**. Above data indicated that compound **2** was an epimer of **1** with the difference being the relative configuration at C-3'. This deduction was further confirmed by the obvious NOE enhancement between H-7 and H-5'. Compound **2** was also isolated as a racemic mixture as confirmed by optical rotation analysis. Thus, the structure of **2** was elucidated as shown in Fig. 1.

Calliviminone E (**3**) was deduced to have a molecular formula of $C_{25}H_{38}O_3$, on the basis of the HRESIMS data showing a pseudomolecular ion at m/z 387.2893 $[M+H]^+$ (calcd. 387.2894). The 1H and ^{13}C NMR data for compound **3** showed signals characteristic of a syncarpic acid system⁶ [δ_H 1.37, 1.39, 1.39, 1.33 (each 3H, s) and δ_C 213.0, 208.3, 208.2, 67.7, 56.9, 56.3, 26.2, 26.0, 25.1, 24.3], a myrcene moiety [δ_H 5.30 (1H, br s), 5.03 (1H, t, $J=7.0$), 2.49 (1H, dd, $J=17.5, 1.5$), 2.16 (1H, m), 2.14 (1H, m), 2.02 (1H, m), 2.04 (2H, m), 1.94 (2H, m), 1.67 (3H, s), 1.59 (3H, s)] and a disubstituted isopentyl group [δ_H 2.30 (1H, m), 1.42 (1H, m), 0.79 (1H, m), 1.64 (1H, m), 0.86 (3H, t, $J=7.0$) 0.85 (3H, d, $J=7.0$)]. The HMBC correlations (Figure 3) of H-8/C-7, H-7/C-3', H-1'/C-6 and C-1, H-5'/C-4' and C-2' indicated that compound **3** was an adduct of syncarpic acid derivative and myrcene.⁶ HMBC cross-peaks of C-6 with H-7, H-2-1', H-3-15 and H-3-12 established that the myrcene unit was linked to the

syncarpic acid nucleus via a quaternary spirocenter at C-6. Above data indicated that the syncarpic acid derivative connected with monoterpene moiety via carbon Diels-Alder manner. A comparison of the NMR data (Table 1) of **3** with those of calliviminone A⁶ suggested that **3** shared the same skeleton with calliviminone A, except for the disubstituted isobutyl chain in calliviminone A was replaced by the disubstituted isopentyl chain in **3**. This was further confirmed by the HMBC correlations of H-8/C-7, C-11, and C-10. Due to the lack of optical rotation value, **3** was a racemic mixture with the stereogenic center at C-7. Based on the above deductions, the planar structure of **3** was established as shown in Figure 1, which possessed spiro-[5.5] undecene skeleton constructed of an isopentyl syncarpic acid and a myrcene moieties.

The molecular formula of compound **4** was calculated to be C₂₅H₃₈O₃ on the basis of the HRESIMS data showing a pseudomolecular ion at m/z 387.2890 [M+H]⁺ (calcd. 387.2894). The IR, NMR and UV data of **4** were closely comparable to those of **3**, suggested that both compounds have the same spiro-[5.5] undecene skeleton. The only difference between these compounds was shown to be the location of the substituent. This different between **3** and **4** could be due to the regioselectivity in [4+2]-cycloaddition. Comparison of the NMR data (Table 1) with those of **3** revealed the chemical shifts of C-1' ($\Delta\delta$ -2.6), C-2' ($\Delta\delta$ 1.2), C-3' ($\Delta\delta$ -2.4), which suggested that syncarpic acid (β -triketones) moiety conjugated with myrcene via a *para* orientation in **4**, rather than *meta* orientation in **3**. This was further confirmed by the HMBC correlations of H-5' (δ_H 2.02) with C-4' (δ_C 29.8), H-1' (δ_H 1.95) with C-8 (δ_C 38.0), H-4' (δ_H 2.47) with C-1 (δ_C 208.5) and C-6 (δ_C 69.0). In addition, compound **4** was also a racemic mixture without optical rotation value. Hence, the structure of **4** was elucidated as shown.

Calliviminone G (**5**) is an isomer of **3**, as deduced from HRESIMS spectrum ([M+H]⁺ m/z 387.2895, calcd. 387.2894). The ¹H and ¹³C NMR data (Table 2) for compound **5** showed signals characteristic of a syncarpic acid system and a myrcene

unit, already observed in compounds **3** and **4**. The ^1H NMR spectrum also showed one doublet methyl at δ_{H} 0.84 (d, $J=7.0$ Hz, Me-11), one triplet methyl at δ_{H} 0.81 (t, $J=7.0$ Hz, Me-10), two methines at δ_{H} 2.28 (m, H-7) and 1.43 (m, H-8), and one methylene at δ_{H} 1.52 (m, H-9) and 1.03 (m, H-9), suggested the presence of a disubstituted 2-methylbutyl group. The HMBC correlations (Figure 4) of H-8/C-7, H-7/C-3', H-1'/C-6 and C-1, H-5'/C-4' and C-2' indicated that compound **5** was also an adduct of syncarpic acid derivative and myrcene in carbon Diels-Alder manner. Moreover, the NMR spectroscopic data and HMBC correlations observed for **5** mostly exhibited the same results as for **3** except for the replacement of the disubstituted isopentyl resonances by disubstituted 2-methylbutyl resonances. This was further confirmed by the triplet of Me-10 (doublet for **3**) and the HMBC correlations of H-8/C-7, C-11, and C-10. Based on the above deductions, the planar structure of **5** was established as depicted in Figure 1, which possessed spiro-[5.5] undecene skeleton constructed of a 2-methylbutyl syncarpic acid and a myrcene moieties.

The relative configuration of C-7 and C-8 was unable to be established by NOE experiment due to the conformational flexible chain. However, different from compounds **1-4**, **5** was obtained as a single-isomer with the obvious Cotton effects in CD spectrum and optical rotation. Therefore, the calculated CD spectrum method was applied to determining the absolute configuration of **5**. Good qualitative matching result between the calculated CD spectrum of the 7*S*, 8*S* isomer and the measured ones (Figure 5) led to the conclusion that the absolute configuration of **5** was 7*S*, 8*S*.

Calliviminone H (**6**), with a molecular formula $\text{C}_{25}\text{H}_{38}\text{O}_3$ had the same planar structure as **5**, as confirmed by extensive 2D NMR analysis (Figure S6.3–6.5 in Supporting Information). However, compared with **5**, differences of the chemical shifts of C-9 ($\Delta\delta$ +5.4), C-11 ($\Delta\delta$ -4.3), C-1' ($\Delta\delta$ -1.3), C-2' ($\Delta\delta$ +1.0) were observed in ^{13}C NMR spectrum of **6** (Table 2), which suggested that **6** was a diastereoisomer of **5** with the difference being the configuration at C-7. From a biosynthetic point of view, the configurational distinctions of **5** and **6** could be attributed to the

stereoselectivity in [4+2]-cycloaddition. The presence of the chiral carbon in the 2-methylbutyl chain led to the separation of compounds **5** and **6**. Furthermore, the CD spectrum of **6** was of a mirror-image type in comparison with the spectrum of **5** (Figure 5). Thus, the absolute configuration of **6** was assigned as 7*R*, 8*S* by comparing the CD spectrum of **5**.

Based on the structural features of calliviminones C-H (**1-6**), their biosynthetic pathway was proposed as depicted in scheme 1. According to the hypothesis, the hetero- or carbon-Diels-Alder reactions between β -triketone derivative and myrcene units play the key role in formation of these novel adducts. Compounds **1-4** were isolated as racemic mixtures, which indicated that the [4+2] cycloaddition had proceeded by a pathway in which the steric hindrance for diene attacking to dienophile via an *anti* or *syn* orientation was indistinguishable. The Diels-Alder reaction has two possible suprafacial approaches (*endo* and *exo*), which led to the difference between **1** and **2**. On the other hand, the plausible biosynthetic pathway for compounds **3-6** was deduced through carbon Diels-Alder reaction. The different structures of **3** and **4** was due to the regioselectivity in [4+2]-cycloaddition, as we have previously reported.^{6, 9} The presence of the chiral carbon in the disubstituted 2-methylbutyl chain and the stereoselectivity in carbon-Diels-Alder reaction account for the isolation of compounds **5** and **6** as a single diastereomer, respectively.

All compounds were evaluated for their inhibitory effects on the NO production in LPS-induced RAW264.7 macrophage cells.¹⁰ Cell viability assay results indicated that none of the test compounds showed evident cytotoxicity at their effective concentrations. Compounds **2-6** exhibited inhibitory effects against NO production with IC₅₀ values ranging between 19.9 \pm 1.0 μ M for **6** and 48.6 \pm 3.1 μ M for **5** (Table 3). The moderate to weak activities of **1** and **5** are lower in comparison to those of **2** and **6**, respectively, inspired us to presume that the stereochemistry of **1**, **2**, **5**, and **6** could affect their inhibition activities. Compounds **3** and **4** also exhibited moderate activities, with IC₅₀ values of 27.6 \pm 5.5 and 35.6 \pm 0.8 μ M, respectively. These values are in the

same range as the previous described activities of calliviminones A and B.⁶ On the basis of these biological results, we hypothesize that the location of the C-3'-C-10' side chain had no obvious effect on the inhibition activity.

In short, a further phytochemical investigation of the fruits of *C. viminalis* led to the discovery of six novel polymethylated phloroglucinol-monoterpene adducts. Compounds **1-4** were obtained as racemic mixtures without the optical rotations and obvious Cotton effects in CD spectrum.^{6, 10-13} **5** and **6** were isolated as optically pure compounds due to the presence of the chiral carbon in the disubstituted 2-methylbutyl chain. Moreover, calliviminones C and D (**1-2**) represent an unprecedented skeleton resulted from the conjugation of β -triketone derivative and monoterpene (myrcene) units via hetero-Diels-Alder reaction. **5** and **6** represent the first examples of diastereomerically pure adduct with an unusual spiro-[5.5] undecene skeleton. Furthermore, the unambiguous determination of the absolute configuration of compounds **5** and **6** will provide valuable data for future research on this type of rare phloroglucinol-terpene adducts. Above results indicated that Diels-Alder reaction may play an important role in the biosynthetic process of secondary metabolites of plant from the genus *Callistemon*.

EXPERIMENTAL SECTION

General Experimental Procedures. Optical rotations were measured with a JASCO P-1020 polarimeter. UV spectra were performed on a Shimadzu UV-2450 spectrophotometer. ECD spectra were obtained on a JASCO 810 spectropolarimeter (JASCO, Tokyo, Japan). IR spectra were recorded on a Bruker Tensor 27 spectrometer with KBr-disks. NMR spectra were acquired on Bruker Avance III-500 instrument (¹H: 500 MHz, ¹³C: 125 MHz), with TMS as internal standard. HRESI mass spectra were recorded on an Agilent 6520B Q-TOF mass instrument. Silica gel (100–200 and 200–300 mesh, Qingdao Haiyang, Qingdao, People's Republic of

China), Sephadex LH-20 (Pharmacia, Uppsala, Sweden), and RP-C₁₈ (40–63 μ m, Fuji, Tokyo, Japan) were used for column chromatography. Analytical HPLC was measured on an Agilent 1200 Series instrument with a DAD detector using a shim-pack VP –ODS column (250 \times 4.6 mm). Preparative HPLC was carried out using Shimadzu LC-6A instrument with a shim-pack RP-C₁₈ column (20 \times 200 mm) and a SPD-10A detector. All solvents were of analytical grade.

Plant Material. The fruits of *Callistemon viminalis* were collected from Guangdong province of China in April 2014, and identified by Professor Minjian Qin, China Pharmaceutical University. A voucher specimen (No.CV-201404) was deposited in the Department of Natural Medicinal Chemistry, China Pharmaceutical University.

Extraction and Isolation. Air-dried and powdered fruits of *Callistemon viminalis* (5.0 kg) were ground and extracted with CH₂Cl₂ (3 \times 4 h) by percolation at room temperature to give 110 g of dried extract. The extract was subjected to silica gel column chromatography using a step gradient of petroleum ether/EtOAc (10:1 to 1:1) to yield four main fractions (Fr. A–D) based on TLC analysis.

Fraction A (9.0 g) was then applied onto an ODS column using a step gradient of MeOH–H₂O (70:30 to 100:0), to give eight subfractions (Fr. A.1–8). Fr. A.4 was subjected to passage over a column of Sephadex LH-20 eluted with MeOH to give two subfractions (Fr. A.4.1-2). Fr. A.4.2 was purified by preparative HPLC with MeOH–H₂O (90:10, 10 mL/min) as the mobile phase to give **3** (4 mg), **4** (3 mg), **5** (3 mg), **6** (4 mg). Fr. A.3 was subjected to separation over Sephadex LH-20 and then preparative HPLC with MeOH–H₂O (85:15, 10 mL/min) to yield **1** (2 mg) and **2** (3 mg).

Calliviminone C (1): colorless gum, $[\alpha]_D^{27} \pm 0$ (c 0.08, MeOH); UV (MeOH) λ_{\max} (log ϵ) 264 (3.84), 203 (3.60) nm; IR (KBr) ν_{\max} 3443, 2958, 2926, 2871, 1714, 1646, 1613, 1463, 1383 cm⁻¹; ¹H and ¹³C NMR data, see Table 1; HRESIMS m/z 373.2738

$[M+H]^+$ (calcd. for $C_{24}H_{37}O_3$ 373.2737).

Calliviminone D (2): colorless gum, $[\alpha]_D^{27} \pm 0$ (c 0.11, MeOH); UV (MeOH) λ_{\max} (log ϵ) 264 (3.91), 203 (3.64) nm; IR (KBr) ν_{\max} 3444, 2960, 2926, 2872, 1716, 1647, 1609, 1460, 1380 cm^{-1} ; ^1H and ^{13}C NMR data, see Table 1; HRESIMS m/z 373.2735 $[M+H]^+$ (calcd. for $C_{24}H_{37}O_3$ 373.2737).

Calliviminone E (3): colorless gum, $[\alpha]_D^{27} \pm 0$ (c 0.042, MeOH); UV (MeOH) λ_{\max} (log ϵ) 205 (3.66) nm; IR (KBr) ν_{\max} 3450, 2956, 2926, 2850, 1698, 1632, 1465, 1384 cm^{-1} ; ^1H and ^{13}C NMR data, see Table 1; HRESIMS m/z 387.2893 $[M+H]^+$ (calcd. for $C_{25}H_{39}O_3$ 387.2894).

Calliviminone F (4): colorless gum, $[\alpha]_D^{27} \pm 0$ (c 0.08, MeOH); UV (MeOH) λ_{\max} (log ϵ) 205 (3.75) nm; IR (KBr) ν_{\max} 3449, 2957, 2926, 2870, 1698, 1632, 1464, 1383 cm^{-1} ; ^1H and ^{13}C NMR data, see Table 1; HRESIMS m/z 387.2890 $[M+H]^+$ (calcd. for $C_{25}H_{39}O_3$ 387.2894).

Calliviminone G (5): colorless gum, $[\alpha]_D^{26} -13.8$ (c 0.22, MeOH); UV (MeOH) λ_{\max} (log ϵ) 205 (3.67) nm; CD (MeOH) 284 ($\Delta\epsilon$ -1.7), 232 ($\Delta\epsilon$ +2.9); IR (KBr) ν_{\max} 3444, 2959, 2923, 2877, 1713, 1632, 1458, 1381 cm^{-1} ; ^1H and ^{13}C NMR data, see Table 2; HRESIMS m/z 387.2895 $[M+H]^+$ (calcd. for $C_{25}H_{39}O_3$ 387.2894).

Calliviminone H (6): colorless gum, $[\alpha]_D^{26} +14.7$ (c 0.21, MeOH); UV (MeOH) λ_{\max} (log ϵ) 205 (3.60) nm; CD (MeOH) 283 ($\Delta\epsilon$ +1.6), 228 ($\Delta\epsilon$ -2.4); IR (KBr) ν_{\max} 3439, 2962, 2929, 2876, 1698, 1630, 1463, 1382 cm^{-1} ; ^1H and ^{13}C NMR data, see Table 2; HRESIMS m/z 387.2892 $[M+H]^+$ (calcd. for $C_{25}H_{39}O_3$ 387.2894).

NO Production Bioassay. The protocol for NO production bioassays was provided in previously published papers.^{6, 14} N-monomethyl-L-arginine was used as the positive control. All experiments were performed in three replicates.

Quantum Chemical ECD Calculation. The conformational analysis was performed by means of the semi-empirical PM3 method, as implemented in the

Gaussian 09 program package¹⁵ starting from preoptimized geometries generated by the MM2 force field in ChemBio3D software overlaid with key correlations observed in the ROESY spectrum. The corresponding minimum geometries found were further optimized by DFT calculations at the B3LYP/6-31G (d,p) level, leading to two minimum structures in both cases. For these geometries, ECD computations were performed by means of the TDDFT [B3LYP/6-31G (d,p)] method. The rotatory strengths were summed, and energetically weighted according to the Boltzmann statistics. The GaussSum was used for visualization of the results.¹⁶

ASSOCIATED CONTENT

Supporting Information. 1D NMR, 2D NMR spectra and HRESIMS data of **1-6** and CD spectra of **5** and **6** are available free of charge via the Internet at <http://pubs.acs.org>.

AUTHOR INFORMATION

Corresponding Author

*Tel/Fax: +86-25-8327-1405. E-mail: cpu_lykong@126.com (L.-Y. Kong).

Notes

The authors declare no competing financial interest.

ACKNOWLEDGMENTS

This research work was financially supported by the National Natural Sciences Foundation of China (81430092), the Program for New Century Excellent Talents in University (NCET-2013-1035), the Program for Changjiang Scholars and Innovative

Research Team in University (PCSIRT-IRT1193), and the Project Funded by the Priority Academic Program Development of Jiangsu Higher Education Institutions (PAPD).

REFERENCES

1. I. P. Singh and S. P. Bharate, *Nat. Prod. Rep.*, 2006, **23**, 558–591.
2. State Administration of Traditional Chinese Medicine of the People's Republic of China, *Chinese Materia Medica*, Shanghai Scientific and Technical Publishers, Shanghai, 1999, 15, 4711.
3. M. Lounasmaa, H. Puri, C. Widen, *Phytochemistry*, 1977, **16**, 1851-1852.
4. B. P. S. Khambay, D. G. Beddie, A. M. Hooper, M. S. J. Simmonds and P. W. C. Green, *J. Nat. Prod.*, 1999, **62**, 1666-1667.
5. S. Rattanaburi, W. Mahabusarakam, S. Phongpaichit and A. R. Carroll, *Tetrahedron*, 2013, **69**, 6070-6075.
6. L. Wu, J. Luo, Y. Zhang, M. Zhu, X. Wang, J. Luo, M. Yang, B. Yu, H. Yao, Y. Dai, Q. Guo, Y. Chen, H. Sun and L. Kong, *Tetrahedron Lett.*, 2015, **56**, 229-232.
7. A. R. Carroll, V. M. Avery, S. Duffy, P. I. Forster and G. P. Guymer, *Org. Biomol. Chem.*, 2013, **11**, 453.
8. F. Cottiglia, L. Casu, M. Leonti, P. Caboni, C. Floris, B. Busonera, P. Faarci, A. Ouhtit and G. Sanna, *J. Nat. Prod.*, 2012, **75**, 225-229.
9. F. Fringuelli, A. Taticchi, *The Diels-Alder Reaction. Selected Practical Methods*, Wiley, Chichester, 2002, pp. 22-23.
10. M. Hans, M. Charpentier, V. Huch, J. Jauch, T. Bruhn, G. Bringmann, D. Quandt, *J. Nat. Prod.*, 2015, in press, DOI: 10.1021/acs.jnatprod.5b00358.
11. D. Tapiolas, B. Bowden, E. Mansour, R. Willis, J. Doyle, A. Muirhead, C. Liptrot, L. Llewellyn, C. W. Wolff, A. Wright, C. Motti, *J. Nat. Prod.*, 2009, **72**,

- 1115-1120.
12. Y. Gao, G. Wang, K. Wei, P. Hai, F. Wang, J. Liu, *Org. Lett.*, 2012, **14**, 5936-5939.
13. M. Takasaki, T. Konoshima, M. Kozuka, M. Haruna, K. Ito, S. Yoshida, *Chem. Pharm. Bull.*, 1994, **42**, 2177-2179.
14. (a) H. J. Zhang, J. Luo, S. M. Shan, X. B. Wang, J. G. Luo, M. H. Yang and L. Y. Kong, *Org. Lett.*, 2013, **15**, 5512-5515. (b) G. Laverny, G. Penna, M. Uskokovic, S. Marczak, H. Maehr, P. Jankowski, C. Ceailles, P. Vouros, B. Smith, M. Robinson, G. S. Reddy, L. Adorini, *J. Med. Chem.*, 2009, **52**, 2204-2213.
15. M. J. Frisch, G. W. Trucks, H. B. Schlegel, G. E. Scuseria, M. A. Robb, J. R. Cheeseman, G. Scalmani, V. Barone, B. Mennucci, G. A. Petersson, H. Nakatsuji, M. Caricato, X. Li, H. P. Hratchian, A. F. Izmaylov, J. Bloino, G. Zheng, J. L. Sonnenberg, M. Hada, M. Ehara, K. Toyota, R. Fukuda, J. Hasegawa, M. Ishida, T. Nakajima, Y. Honda, O. Kitao, H. Nakai, T. Vreven, J. A. Jr. Montgomery, J. E. Peralta, F. Ogliaro, M. Bearpark, J. J. Heyd, E. Brothers, K. N. Kudin, V. N. Staroverov, R. Kobayashi, J. Normand, K. Raghavachari, A. Rendell, J. C. Burant, S. S. Iyengar, J. Tomasi, M. Cossi, N. Rega, J. M. Millam, M. Klene, J. E. Knox, J. B. Cross, V. Bakken, C. Adamo, J. Jaramillo, R. Gomperts, R. E. Stratmann, O. Yazyev, A. J. Austin, R. Cammi, C. Pomelli, J. W. Ochterski, R. L. Martin, K. Morokuma, V. G. Zakrzewski, G. A. Voth, P. Salvador, J. J. Dannenberg, S. Dapprich, A. D. Daniels, O. Farkas, J. B. Foresman, J. V. Ortiz, J. Cioslowski, D. J. Fox, Gaussian 09, Revision B. 01, Gaussian Inc., Wallingford, CT, 2010.
16. N. M. O'boyle, A. L. Tenderholt, K. M. Langner, *J. Comput. Chem.*, 2008, **29**, 839-845.

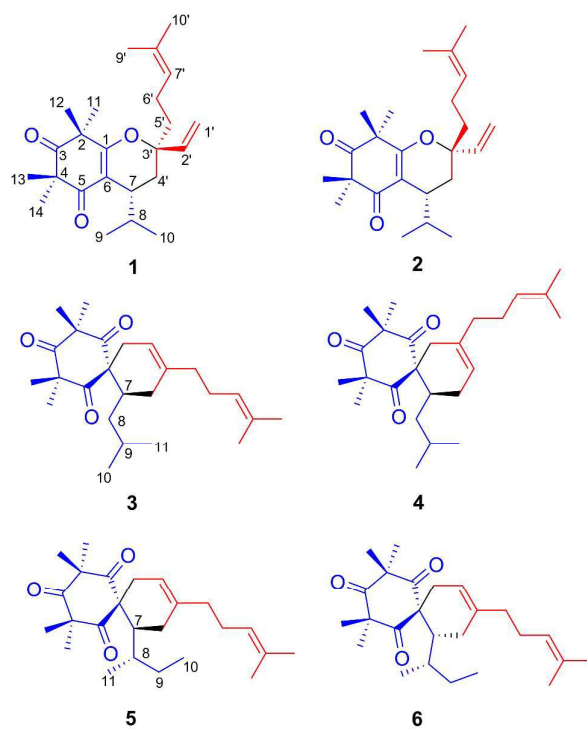


Figure 1. Structures of compounds 1-6

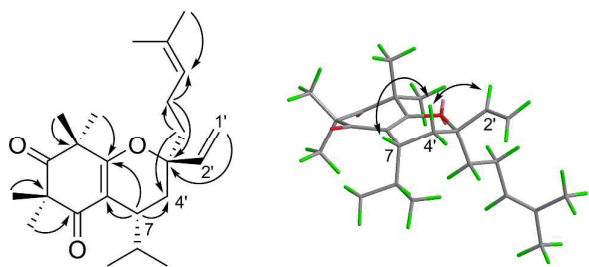


Figure 2. Key HMBC and ROESY correlations of compound **1**

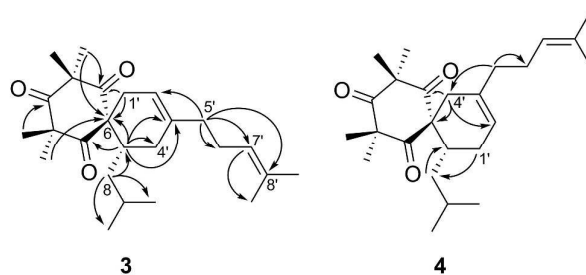


Figure 3. Key HMBC (\rightarrow) correlations of compounds **3** and **4**

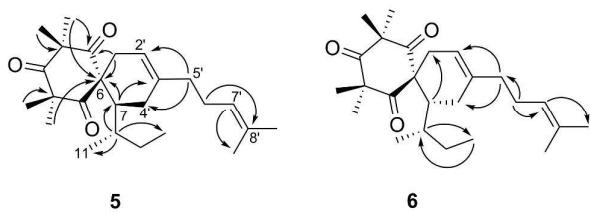


Figure 4. Key HMBC (→) and ROESY (↔) correlations of compounds **5** and **6**

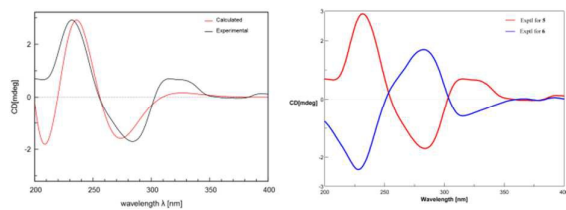


Figure 5. Calculated and experimental ECD spectra of (7*S*, 8*S*)-**5** and comparison of the experimental ECD spectra of **5** and **6**.

Scheme 1. The Plausible Biogenetic Pathway for **1-6**

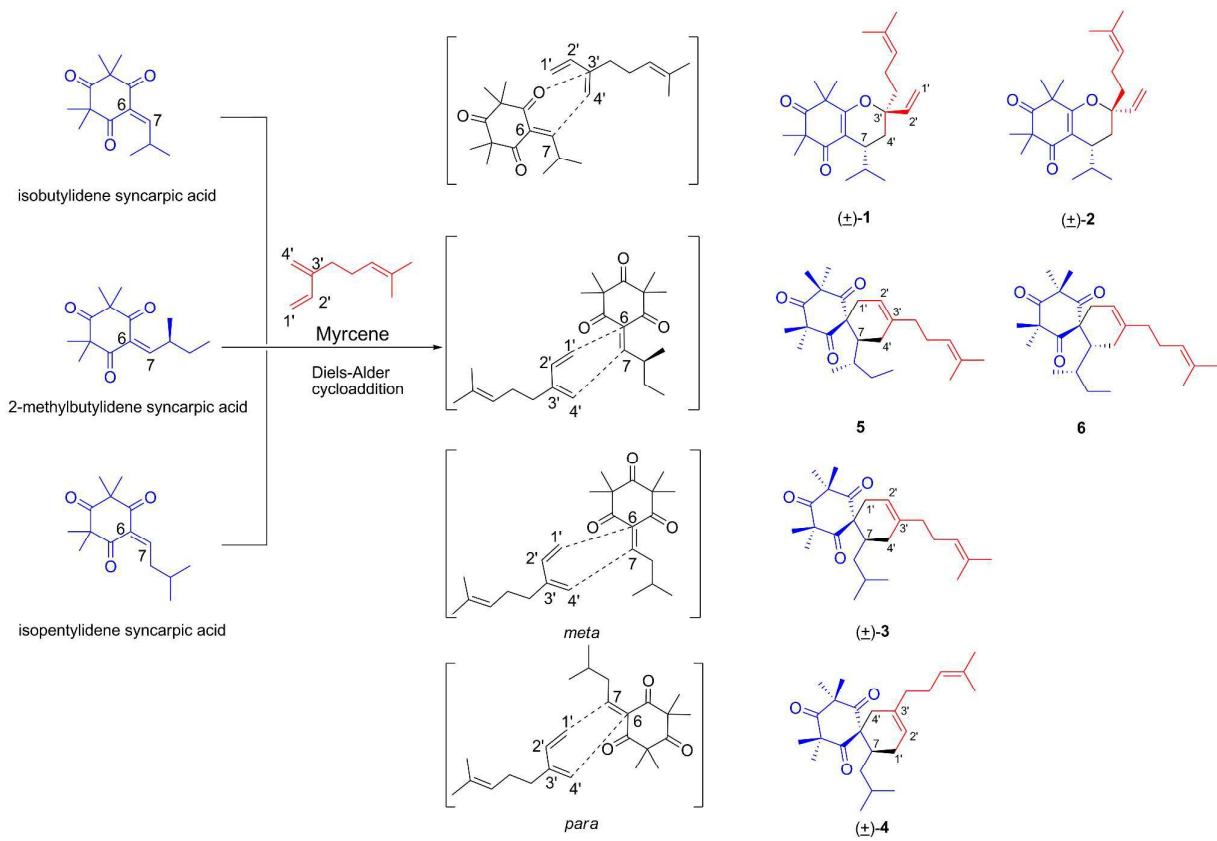


Table 1. ^1H (500 MHz) and ^{13}C (125 MHz) NMR Spectroscopic Data for **1–4** in CDCl_3

Position	1		2		3		4	
	δ_{H} (J in Hz)	δ_{C}	δ_{H} (J in Hz)	δ_{C}	δ_{H} (J in Hz)	δ_{C}	δ_{H} (J in Hz)	δ_{C}
1		170.7		169.8		208.3		208.5
2		48.3		48.6		56.9		56.3
3		213.6		213.4		213.0		213.2
4		55.6		55.5		56.3		56.1
5		197.7		198.1		208.2		208.2
6		112.5		112.0		67.7		69.0
7	2.62, m	33.4	2.71, m	33.3	2.30, m	34.1	2.20, m*	33.7
8	2.71, m	26.1	2.60, m	26.7	1.42, m	39.3	1.32, m*	38.0
					0.79, m		0.71, m	
9	0.95, d (7.0)	20.8	0.91, d (7.0)	20.8	1.64, m*	25.6	1.58, m	25.6
10	0.60, d (7.0)	15.6	0.65, d (7.0)	16.4	0.86, d (7.0)	24.4	0.85, d (6.5)	24.3
11	1.44, s	25.8	1.47, s	24.8	0.85, d (7.0)	21.0	0.81, d (6.5)	21.1
12	1.40, s	25.3	1.37, s	26.2	1.39, s	26.0	1.43, s	26.1
13	1.31, s	24.0	1.34, s	23.0	1.37, s	24.3	1.37, s	25.8
14	1.30, s	25.2	1.33, s	26.1	1.39, s	25.1	1.41, s	24.4
15					1.33, s	26.2	1.32, s	26.7
1'	5.07, d (17.5)	115.4	5.31, d (17.5)	113.7	2.49, dd (17.5, 1.5)	29.6	1.95, m*	27.0
	5.16, d (11.0)		5.21, d (11.0)		2.16, m*			
2'	5.63, dd (17.5, 11.0)	139.1	5.93, dd (17.5, 11.0)	140.9	5.30, br s	116.0	5.24, br s	117.2
3'		81.8		81.2		136.8		134.4
4'	1.89, dd (14.0, 7.0)	29.8	1.84, dd (14.0, 6.5)	30.7	2.14, m*	30.8	2.47, d (18.0)	29.8
	1.61, m		1.64, m*		2.02, m*		2.07, m*	
5'	1.72, m	41.7	1.64, m*	36.0	1.94, m	37.3	2.02, m*	37.4
			1.51, m					
6'	2.15, m	22.0	1.96, m	22.4	2.04, m*	26.4	2.12, m*	26.3
	2.07, m							
7'	5.13, t (7.0)	123.9	5.00, t (7.0)	123.6	5.03, t (7.0)	124.1	5.08, t (7.0)	124.1
8'		132.1		132.3		131.7		131.7
9'	1.69, s	25.8	1.65, s	25.7	1.67, s	25.8	1.67, s	25.8
10'	1.62, s	17.7	1.55, s	17.7	1.59, s	17.8	1.61, s	17.8

* indicate overlapped signals.

Table 2. ¹H (500 MHz) and ¹³C (125 MHz) NMR Spectroscopic Data for **5** and **6** in CDCl₃

Position	5		6	
	δ_{H} (<i>J</i> in Hz)	δ_{C}	δ_{H} (<i>J</i> in Hz)	δ_{C}
1		209.2		209.0
2		57.0		56.9
3		212.9		212.7
4		56.8		56.9
5		208.7		208.5
6		66.3		66.8
7	2.28, m*	41.4	2.29, m*	40.7
8	1.43, m*	37.8	1.36, m*	36.6
9	1.52, m 1.03, m	25.5	1.25, m	30.9
10	0.81, t (7.0)	12.3	0.84, t (7.5)	12.2
11	0.84, d (7.0)	19.8	0.79, d (7.0)	15.5
12	1.41, s	26.5	1.42, s	26.3
13	1.39, s	25.8	1.38, s	24.9
14	1.34, s	25.7	1.33, s	24.8
15	1.39, s	24.7	1.38, s	26.0
1'	2.41, dd (17.5, 4.5) 2.15, m*	32.9	2.50, dd (17.5, 2.0) 2.21, m	31.6
2'	5.21, br s	114.6	5.27, br s	115.6
3'		139.4		138.3
4'	2.28, m* 2.09, m*	29.3	2.24, m* 1.93, m	27.5
5'	1.97, m	37.2	1.97, m	37.3
6'	2.07, m*	26.3	2.07, m	26.4
7'	5.04, t (7.0)	124.2	5.05, t (7.0)	124.3
8'		131.6		131.6
9'	1.67, s	25.8	1.67, s	25.8
10'	1.59, s	17.8	1.59, s	17.8

* indicate overlapped signals.

Table 3. The Inhibitory Activities on Nitric Oxide (NO) Production of **1-6**.

Compound	IC ₅₀ ± SD (μM) ^a
1	>50
2	35.6 ± 0.8
3	27.6 ± 5.5
4	30.8 ± 5.5
5	48.6 ± 3.2
6	19.9 ± 1.0
L-nmma	44.0 ± 5.64

^aValues present mean ± SD of triplicate experiments.